

# Exhumation and Basin Development Related to Formation of the Central Andean Plateau, 21° S

Ekkehard Scheuber · Dorothee Mertmann · Harald Ege · Patricio Silva-González · Christoph Heubeck  
Klaus-Joachim Reutter · Volker Jacobshagen

**Abstract.** Thermochronological (apatite fission track, AFT) and sedimentological data from the central Andean high plateau and its eastern foreland reflect the Tertiary tectonic evolution of this plateau. AFT data define several stages of exhumational cooling in the plateau and its foreland: A first stage (AFT dates of 40 and 36 Ma), restricted to the central Eastern Cordillera, can be attributed to initial thrusting increments following the Incaic Phase. Around 33–30 Ma, cooling occurred along basement highs over the entire plateau; kinematics were thrusting (eastern Cordillera) as well as normal faulting (Altiplano). From 17 Ma onwards, exhumational cooling took place in the eastern foreland (Interandean-Subandean), reflecting the eastward migration of the thrust front into the Chaco foreland basin.

Sedimentary data agree with the AFT data. Before 32 Ma, fine-grained playa-mudflat deposits indicate tectonic quiescence in most parts of the endorheic basin. Around 32 Ma, a strong change to coarse clastics took place. Between 32 and 18 Ma, alluvial fans and fluvial deposits formed adjacent to fault-bound basement highs. Later growth strata indicate thrusting activity. Since about 10 Ma, flat-lying continental deposits indicate tectonic quiescence from the Altiplano to the Eastern Cordillera, whereas in the Chaco the present foreland was created.

The data are discussed in terms of the development of the active continental margin and a possible scenario is suggested: The Incaic Phase (45–38 Ma) might have been linked to a slab breakoff and subsequent flat slab conditions. During the associated gap in volcanism (38–28 Ma), flat slab subduction may have caused hydration of the upper plate mantle and the initial formation of the plateau. Later plateau uplift could have been caused by crustal thickening owing to tectonic shortening, first within the plateau and its foreland and, since about 10 Ma, in the foreland only.

## 13.1 Introduction

It is generally accepted that the formation of the Altiplano-Puna Plateau resulted from the convergence of the Farallon and Nazca Plates with the South American Plate. Gephart (1994), for example, has shown that both Andean topography and slab geometry are highly symmetrical around a vertical NNE-trending plane that corresponds to the Euler equator and to the Farallon Euler pole of approximately 35 million years ago. Small-scale asymmetries in topography and slab geometry have been attributed to the shifting of the Euler pole after 20 Ma. Thus, it is concluded that the initial stages of plateau formation occurred during the late Eocene to early Oligocene.

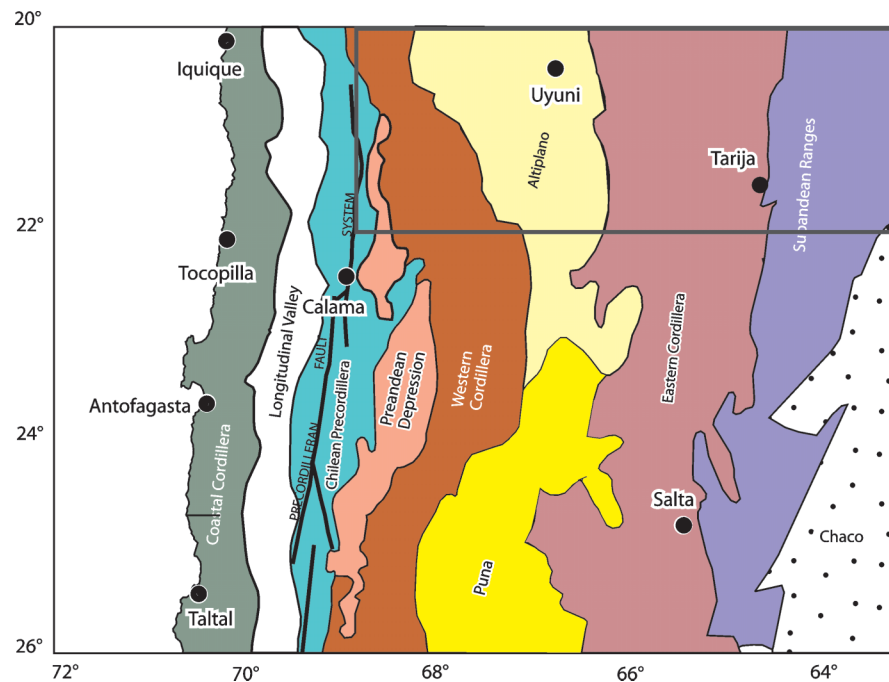
The causes of plateau formation and the single stages of its evolution have, however, remained a matter of debate for a long time. In his widely accepted model, Isacks (1988) assumed that plateau formation started approximately 28 million years ago, caused by processes in the asthenospheric wedge that were effective in thinning the lithospheric mantle of the upper plate. By contrast, James and Sacks (1999) attributed these early stages to a time of flat slab (nearly horizontal) subduction which caused a magmatic pause during much of the Oligocene. Flat slab subduction led to a low geothermal gradient and hydration (serpentinization) of the upper plate mantle, resulting in an early uplift, and extensive shortening deformation in the Eastern Cordillera.

The resumption of volcanism some 28 million years ago indicates the installation of a new asthenospheric wedge beneath the upper plate and, following James and Sacks (1999), a steepening of subduction. In this stage, plateau uplift is assumed to have occurred owing to lithospheric thinning and distributed shortening (pure shear mode) of the upper plate over a “heated and weakened zone” (Isacks 1988). Since 18–12 Ma, the Brazilian shield has been thrust underneath the Andean orogen by transferring the principal location of shortening, first into the Interandean and later into the Subandean Belt (simple shear mode; Baby et al. 1992, 1997; Dunn et al. 1995; Kley 1996; Moretti et al. 1996; DeCelles and Horton 2003; Gubbels et al. 1993). The model of Isacks has been modified by Lamb et al. (1997) and Lamb (2000) for the present stage of the plateau. These authors suggested that the thin-skinned thrusting in the upper crustal foreland is accommodated by ductile distributed shortening beneath the plateau.

The objective of our work is to illuminate the plateau-forming processes in the Central Andes by investigating the geological record within the plateau and its eastern foreland. We have carried out thermochronological, sedimentary and structural work in the plateau and foreland, and have particularly focused on the Tertiary strata of the Altiplano, which we compare with those of the Subandean Zone (Figs. 13.1 and 13.2). The Tertiary Altiplano sediments reflect the tectonic activity of the early

**Fig. 13.1.**

Morphostructural units of the Central Andes. (The box locates the study area of Fig. 13.2)



stages of plateau formation, whereas the basin sediments of the Chaco foreland reflect lithospheric loading of the foreland lithosphere resulting from the thrusting of the Brazilian shield beneath the Andean orogen. Our sedimentological work was accompanied by apatite fission track (AFT, e.g. Wagner and van der Haute 1992) analyses along an E-W traverse at about 21° S, from the Western Cordillera to the Subandean, in order to date the exhumation and uplift history.

### 13.2 Geological Setting

The Central Andes formed in a long-lived convergent setting in which, since the Jurassic, several oceanic plates were subducted beneath the leading edge of the South American Plate. Subduction resulted in the formation of a magmatic arc that, due to tectonic erosion, has migrated about 200 km eastwards since 120 Ma, moving from the Coastal Cordillera to its present position in the Western Cordillera (Fig. 13.1). This volcanic arc is located along the western margin of the Altiplano-Puna Plateau, which (with a mean 3.8 km elevation) mainly belongs to the back-arc region of the Andean arc system, but also comprises the Chilean Precordillera at about 21° S where it forms the western monocline of the plateau (Isacks 1988).

Eastwards, the Altiplano-Puna Plateau is limited by the Eastern Cordillera with elevations exceeding 5000 m. On the eastern slope of the plateau, the (west to east) Interandean and Subandean Belts represent detached and deformed foreland sediments, whereas the Chaco represents

the present foreland basin. The Interandean to Chaco units reflect the lateral growth of the Andean orogen and its thrusting onto the stable Precambrian Brazilian Shield.

In the north Chilean Precordillera, along the western margin of the plateau, rocks and structures of the Palaeogene magmatic arc crop out in orogen-parallel, bivergent ridges and are underlain by Mesozoic formations and a Palaeozoic basement (Günther 2001). Its major structure is the Precordilleran Fault System (PFS), a bivergent, transpressional zone that originated as a trench-linked, strike-slip system within the Eocene magmatic arc (Döbel et al. 1992). Several world-class ore deposits (e.g. Chuquibambata) exist along this fault system.

The Altiplano forms a wide, low-relief and mainly internally-drained basin that is covered by undeformed Upper Miocene to Quaternary volcanics and sediments (Fig. 13.2). This basin is morphologically structured by isolated, N-S- to NNE-SSW-trending ridges with elevations ranging from 4000 m to 5350 m. These are built from Palaeozoic to Neogene strata that, in mid to late Miocene times, underwent dextral transpressional deformation with thrusting toward the east, and have dextral, strike-slip displacements along the Uyuni-Khenayani Fault Zone (UKFZ, Fig. 13.3). The eastern margin of the Altiplano is marked by the San Vicente Fault System (SVFS) where Ordovician sedimentary rocks of the Eastern Cordillera were thrust westwards onto Palaeogene deposits of the Altiplano in the early Miocene (Müller 2000; Müller et al. 2002).

The Eastern Cordillera forms a N-S-trending, bivergent thrust system centered near 65.5° W (Baby et al.

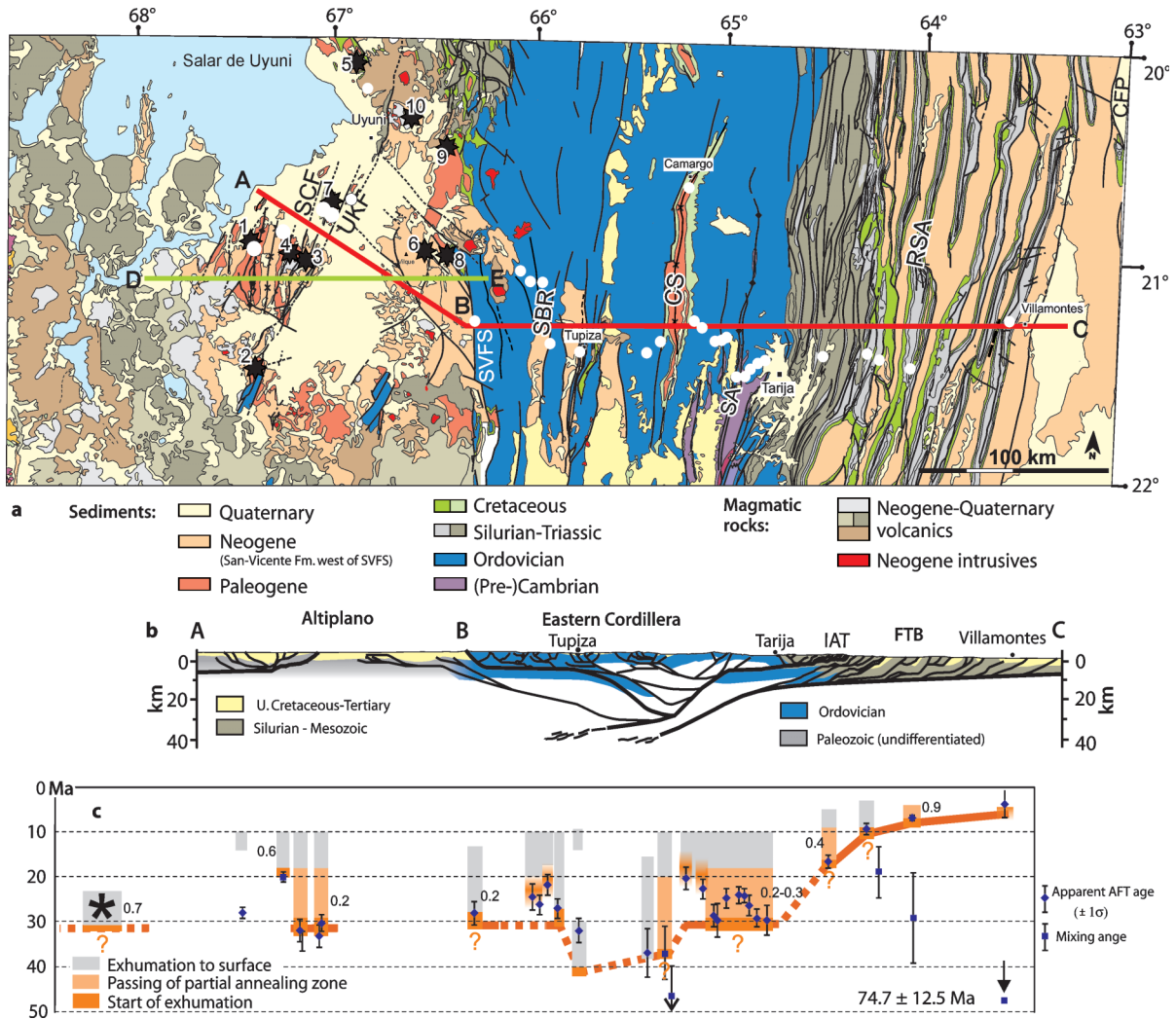


**Fig. 13.2.** a Geological map of the study area: ABC: location of the Apatite fission track thermochronology (AFT) traverse; white dots: AFT sample locations; DE: section of Fig. 13.3; SCF: San Cristobal Fault; UKF: Uyuni-Khenayani Fault; SVFS: San Vicente Fault System; SBR: Santa Barbara Ranges; CS: Camargo Syncline; SA: Sama Anticline; RSA: Rio Salado Anticline; CFP: Cabalgamiento Frontal Principal. Numbered black stars: 1 – Santa Ines, 2 – Cerro Gordo, 3 – San Cristobal 2, 4 – San Cristobal 1, 5 – Chita, 6 – Animas 2, 7 – Corregidores, 8 – Animas 1, 9 – Ubina, 10 – Pulacayo. b Cross section along the AFT traverse ABC. IAT: Interandean Thrust; FTB: Foreland fold-and-thrust belt. c AFT data and modeled cooling and exhumation paths along the cross section: (\*: westernmost data point, assumed source area of crystalline basement pebbles in San Vicente Formation. Numbers refer to averaged exhumation rates in  $\text{mm yr}^{-1}$

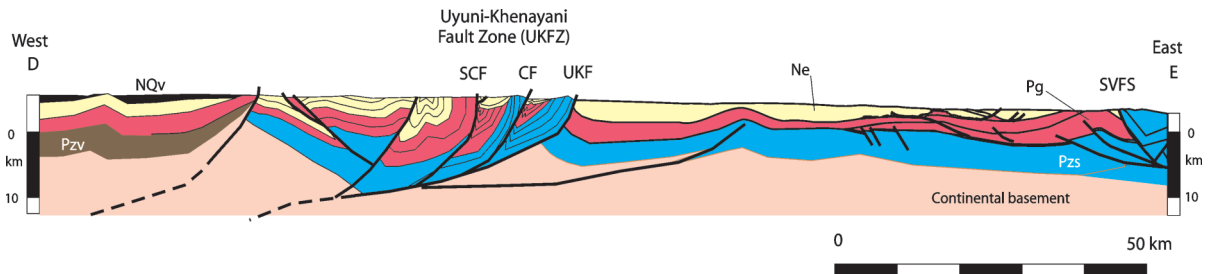


**Fig. 13.3.** Schematic section across the central and eastern Altiplano at  $\sim 21^\circ$  S. For location (D-E) see Fig. 13.2. NQv: Neogene-Quaternary volcanics, Ne: Neogene sediments of the San Vicente Formation, Pg: Paleogene sediments with Upper Cretaceous at the base-Pzv: Palaeozoic volcanics, Pzs: Palaeozoic sediments, SCF: San-Cristobal Fault, CF: Corregidores Fault, UKF: Uyuni-Khenayani Fault

1992, 1996). It is predominantly composed of clastic, metasedimentary rocks of Ordovician age, up to 10 km thick. These rocks are disconformably overlain by either Cretaceous to Palaeocene or mid Tertiary to Neogene sequences. In the late Cretaceous, after mid Cretaceous rifting, a wide, post-rift basin developed which covered large parts of the Eastern Cordillera and the adjacent Altiplano (Sempere 1994; Marquillas and Salfity 1994; Fiedler et al. 2003). Marine deposits of the late Cretaceous and early Tertiary (El Molino Fm.) provide the last regional paleoelevation record prior to Andean deformation (Kley et al. 1997).

During the Eocene and early Oligocene, the central Eastern Cordillera was the source area (Proto-Eastern Cordillera, Lamb et al. 1997) of continental, upwardly coarsening deposits (Potoco and Camargo Fms., Horton and DeCelles 2001; Silva-González 2004) in the eastern Altiplano and in the area of the Camargo syncline (CS in Fig. 13.2). Late Oligocene to Miocene coarse-grained sediments disconformably cover older strata in several N-S-trending intramontane basins (Horton 1998; Kley et al. 1997) that were formed during intense shortening (Horton 1998; Tawackoli 1999, Müller et al. 2002). The formation of a regionally extensive, erosional surface, dating from 13 to 9 Ma, which is covered by undeformed strata, documents the end of deformation in the entire Eastern Cordillera (Gubbels et al. 1993).

Descending to the east, the mean elevation diminishes by about 1500 m to the Interandean and Subandean zones, which form an east-vergent, fold-and-thrust belt and expose Palaeozoic to Mesozoic units. The widely-spaced, thrust-bounded anticlines of the Subandean zone progressively include the Neogene foreland basin sequences of the Chaco and continue eastwards into the undeformed Recent Chaco Basin (Gubbels et al. 1993; Isacks 1988; Kley et al. 1997). At present, approximately half of the original width of the Chaco foreland basin, between the Cabalgamiento Frontal Principal (CFP) in the west and the gentle onlap of flat-lying sediments over the crystalline rocks of the Izozog High (part of the Brazilian Shield) in the east, has been incorporated into the Subandean fold-and-thrust belt; there, shortening reaches approximately 38% (Baby et al. 1992, 1996).

Tectonic shortening thickened the crust to 70 km (Wigger et al. 1994) beneath the Central Andean Plateau. Quantitative analyses of structural profiles across the whole back-arc have revealed that tectonic shortening predominantly occurred during the Cenozoic. For the southern Altiplano, 60–80 km of shortening was calculated (Elger et al. 2005), for the Eastern Cordillera, 90–95 km (Müller et al. 2002), and for the Interandean and Subandean zones, 130–140 km (citations in Müller et al. 2002), although some lower crustal flow out of the section has to be considered (Hindle et al. 2002, 2005).

### 13.3 Exhumation History (Apatite Fission Track Thermochronology)

The exhumation history of the central Andean Plateau has been addressed using AFT thermochronology. A detailed description and interpretation of the AFT data is the focus of another paper (Ege et al. submitted). To date, only a few fission track studies exist from the Altiplano-Puna segment (Benjamin et al. 1987; Kontak et al. 1990; Andriessen and Reutter 1994; Moretti et al. 1996).

Fission tracks in apatite become progressively shorter in the broad temperature range (i.e. 125–60 °C for Durango apatite, Green et al. 1989) of the partial annealing zone (PAZ); a representative number of track lengths measured in a sample can be compared with forward annealing models to constrain the thermal history (e.g. Gallagher 1995). Mean track lengths (MTL) of 14–15 µm indicate rapid cooling, whereas reduced lengths are indicative of longer residence in the PAZ. To address the annealing kinetics of the detrital apatites, the etching parameter “Dpar” was used (Carlson et al. 1999; Ketcham et al. 1999) and thermal models were made with the program “AFTSolve” (Ketcham et al. 2000). For analytical details and modeling parameters, the reader is referred to Ege et al. (2003) and Ege (2004).

Samples from mostly pre-Tertiary sedimentary rocks were collected along a 400 km long transect at ~21° S, extending from the central Altiplano to the Subandean belt (Fig. 13.2), with the aim of characterizing the regional pattern of exhumation. Structurally deep locations, e.g. hanging walls of major thrusts, were preferentially sampled, but, for comparison purposes, some samples were taken from shallower structural positions. A common approach in fission track studies is to take a suite of samples over a range of elevations with the goal of encountering a kink in the age-elevation gradient, marking the time when exhumational cooling began (Benjamin et al. 1987; Fitzgerald et al. 1995). However, owing to low relief and intense deformation within the plateau, such profiles are absent.

Isolated fission track data from buried and subsequently exhumed rocks can provide two different types of information. Where rocks were buried deep enough to exceed the total annealing temperature ( $T_A$ ), the fission track clock was reset to zero and the data record information about the following cooling path. Where  $T_A$  was not achieved, ages and track lengths reflecting the anterior thermal history will be preserved, modified by the final cooling from a maximum temperature lower than  $T_A$ . Small portions of strongly shortened tracks encountered in most samples suggest that they are of the latter type. To distinguish between the two possibilities, the maximum temperature is decisive and is estimated from stratigraphic and structural information, and the assumed paleo-geothermal gradient (see below).

### 13.4 Thermal State of the Crust

Thermal processes might have influenced the observed cooling record. The recent thermal state of the crust is characterized by an elevated heat flow of 100–80 mW m<sup>-2</sup> in the plateau, decreasing to 40 mW m<sup>-2</sup> in the Subandean zone (Springer and Förster 1998). This thermal anomaly has been created by magmatism and crustal thickening since the late Oligocene (Babeyko et al. 2002) and, hence, is coeval with the observed cooling. However, as volcanism started around 28–25 Ma (see below), i.e. later than the observed cooling ages (Fig. 13.2c), a magmatic event that reset the fission track ages can be excluded. Thus, the cooling solely reflects exhumation.

In order to interpret thermochronological data in the spatial frame of reference, the paleo-geothermal gradient has to be assumed. Today, temperature gradients are 39 ± 9 °C km<sup>-1</sup> (±1σ) in the Altiplano, 25 ± 8 °C km<sup>-1</sup> in the Eastern Cordillera and 22 ± 3 °C km<sup>-1</sup> in the Subandean-Chaco (Springer and Förster 1998). A constant geothermal gradient of 25 ± 5 °C km<sup>-1</sup> was assumed for the calculation of exhumation rates (Ege et al. submitted). Given the low amounts and rates of exhumation within the plateau, heat advection by erosion (Brown and Summerfield 1997) is neglected. To relate sediment thickness to temperature, thermal conductivity data from Bolivia were used (Henry and Pollack 1988; Springer 1996).

### 13.5 General Results

In the plateau domain (Altiplano and Eastern Cordillera), apparent cooling ages range between 37 and 20 Ma, with the majority around 30 Ma (Fig. 13.2). The apatite fission tracks exhibit variable amounts of moderate length reduction (< 20%). By contrast, exhumational cooling in the eastern foreland fold-and-thrust belt started much later with cooling ages of 16–9 Ma in the Interandean zone. Mixed ages are obtained in the Subandean zone. Our interpretation of the exhumation history (for details see Ege et al., in prep) is presented below in temporal order.

#### 13.5.1 Late Eocene – Early Oligocene

The earliest cooling along the transect is observed in the central part of the Eastern Cordillera (Fig. 13.2). Near Tupiza, an Ordovician sample (AFT age of 31.5 Ma and MTL of 11.9 μm) was taken below an unconformity with sediments of possible Oligocene age. These sediments are more than 1.2 km thick and were folded in the mid Miocene together with the Ordovician substrate (Kley et al. 1997; Müller et al. 2002). Modeling with corresponding

constraints yielded good fits for a two-phase thermal history with initial cooling since ca. 40 Ma, reheating by burial to about 80 °C, and final cooling to surface temperature after ca. 15 Ma.

The sample from the hanging wall of the Camargo-Yavi Thrust (CYT) which is the western border of the Camargo Syncline (CS, Fig. 13.2) slowly cooled from at least 36 Ma, most likely owing to the initiation of the CYT. Together with an apparent age of 36.4 ± 5.2 Ma from a sample further west, the AFT data from the central Eastern Cordillera delineate a zone of initial and, suggestively, eastwardly propagating uplift in the late Eocene to early Oligocene. Our results are similar to those from the Eastern Cordillera of northern Bolivia where zircon fission track ages indicate the onset of cooling at 45–40 Ma (Benjamin et al. 1987; Lamb and Hoke 1997). We interpret late Eocene exhumation to be contractionally-driven uplift of a narrow proto-Eastern Cordillera and the related inversion of Cretaceous rift structures (Kley et al. 1997; Lamb and Hoke 1997; Hansen and Nielsen 2003).

#### 13.5.2 Oligocene

Widespread cooling occurred within the Oligocene (33–27 Ma) from the Western Cordillera to the eastern margin of the Eastern Cordillera. Apatite crystals from basement pebbles, collected from an early Miocene conglomerate of the San Vicente Fm. in the western Altiplano (Fig. 13.2), yield a uniform cooling age of 28.0 ± 1.2 Ma. The pebbles comprise west-derived, Proterozoic-Palaeozoic, basement rocks (Bahlburg et al. 1986; Wörner et al. 2000). Post-depositional burial of ca. 1 km (Elger et al. 2005) did not heat the sample above 60 °C; the AFT data thus reflect cooling in the source areas of the western Altiplano. In particular, thermal models indicate rapid cooling to less than 145–130 °C since 32–30 Ma.

Four Palaeozoic samples from the hanging walls of two east-vergent thrusts in the Uyuni-Khenayani fault zone (UKFZ, Fig. 13.3) yielded similar AFT cooling ages of between 34 and 30 Ma, but had variable amounts of track shortening. Thermal modeling and the reconstruction of pre-exhumational burial depth indicate maximum temperatures slightly below  $T_A$  with the onset of exhumation occurring between 33 to 29 Ma. Modeled maximum temperatures still require burial heating beneath a thickness of 1.25 ± 0.75 km of early Tertiary sediments (Potoco Fm.).

In principle, the observed exhumational cooling along the UKFZ is compatible with uplift in the footwall of a west-dipping, normal fault (the future San Cristobal thrust, SCF, Figs. 13.2 and 13.3), and also with uplift in the hanging walls of east-vergent, reverse faults (Elger et al. 2005). However, the coarseness of the San Vicente Fm., the abundance of Palaeozoic clasts, even in the basal parts of the San Vicente Fm., and the high sediment thickness west of

the fault rather argue for normal faulting along the SCF during early exhumation (see below).

Until ca. 18 Ma, the Palaeozoic rocks in the UKFZ cooled to a temperature below ~60 °C as exhumational unroofing of 2–3 km occurred, while the Tertiary sample from the basin to the west was continuously heated by sedimentary burial (Fig. 13.2, for details see Ege et al., submitted). Exhumation in this basin started by 20–18 Ma and most likely reflects that the SCF became active as a reverse fault. All samples reached the surface 11–7 million years ago.

In the west-vergent part of the *Eastern Cordillera*, apparent AFT ages range between 28 and 22 Ma. The precise timing of cooling is restricted by incomplete length data and poor constraints on pre-exhumational burial. The stratigraphic throw along the thrust of the San Vicente Fault System (SVFS) of at least 3.8 km (Kley et al. 1997) and the ~2 km thick Palaeogene Potoco Fm. in the footwall (Elger et al. 2005) indicate that the hanging wall sample cooled by about 50 °C prior to its apparent AFT age of 27.7 Ma.

In the western part of the Eastern Cordillera, the fault-bounded Santa Barbara Range (SBR, Fig. 13.2) was exhumed around the same time (AFT age of 26.7 Ma), possibly due to the formation of a fault bend fold at depth (Müller et al. 2002). Samples west of the SBR had shallow positions in the Ordovician stratigraphy (< 1 km), except the sample in the core of the Tres Palcas anticlinal structure (3.9 km). However, the apparent AFT age of the core sample is similar to the sample from the flank (AFT ages of 24.3 Ma and 25.8 Ma, respectively), suggesting that the anticline had mostly formed during the late Palaeozoic. Therefore, samples west of the SBR most likely cooled from a temperature slightly below  $T_A$  some time after their apparent AFT ages, i.e. during the early Miocene.

The exhumation pattern, consistent with relative faulting ages (Müller et al. 2002), indicates that the west-vergent thrust system did not form by in-sequence, propagating deformation, despite the thin-skinned geometry (for discussion see Müller et al. (2002). Earliest exhumation along the SVFS may correlate with the deposition of the alluvial conglomerates of the basal San Vicente Fm., or with the upward coarsening of sediment in the underlying Potoco Fm.

In the eastern part of the Eastern Cordillera, a series of ten lower Ordovician samples have been taken across 1500 m of local relief in the Sama anticlinal structure (SA in Fig. 13.2). These samples yielded cooling ages between 29 and 20 Ma. These data are interpreted to represent the base of a fossil partial annealing zone (for details see Ege et al. submitted). This zone was exhumed by at least 28 Ma, and most likely by 30 Ma. Until ca. 18 Ma, block-like exhumation of 2.8 km was probably achieved by uplift over the ramp of the active main Interandean thrust (IAT).

### 13.5.3 Miocene – Pliocene

Tectonic shortening of the central Altiplano and the Eastern Cordillera occurred until 11–7 Ma (Lamb and Hoke 1997; Müller et al. 2002; Victor et al. 2004; Elger et al. 2005), with bulk shortening rates increasing during the Miocene (Elger et al. 2005). However, the associated rock uplift did not exhumate rocks from below the PAZ after the early Miocene.

The onset of exhumational cooling migrated from the eastern margin of the Eastern Cordillera (Sama anticline) to the east from about 30 Ma, and is clearly linked to the propagation of the deformation front into the eastern foreland. Cooling ages of 16.4 and 9.2 Ma in the central and easternmost part of the *Interandean* zone, respectively, indicate that the exhumational front propagated through this region until about 10 Ma. A sample from the westernmost anticline (mixed age of 28.6 Ma, Fig. 13.2) in the western *Subandean* zone consists of two kinetically different apatite populations; the younger population has a completely reset AFT cooling age of  $6.8 \pm 0.6$  Ma and a MTL of  $13.9 \pm 2.3$   $\mu\text{m}$  that dates the onset of exhumational cooling by 8 Ma, owing to the formation of the anticline. AFT data from the easternmost Subandean anticline near Villamontes (mixed age of 74.7 Ma, Fig. 13.2), cannot constrain the onset of cooling, but suggest that cooling started considerably after 8 Ma. The onset of cooling in the Subandean is clearly reflected in a change in sedimentation (see below).

### 13.5.4 Exhumation Rates and Surface Uplift

Apparent mean exhumation rates were calculated either from the portion of modeled cooling paths hotter than 60 °C or with respect to the surface temperature (15 °C), but only where the timing is constrained and assuming a constant geothermal gradient of  $25 \pm 5$  °C  $\text{km}^{-1}$  (Fig. 13.2). Within the plateau, mean apparent exhumation rates were predominantly low (0.1–0.3  $\text{mm yr}^{-1}$ ) between 33 and 18 Ma (Fig. 13.2). Exceptionally high apparent exhumation rates of 0.6–0.9  $\text{mm yr}^{-1}$  are observed in samples from the basement of the western Altiplano/Western Cordillera. There, notable late Eocene-Oligocene exhumation (Maksaev and Zentilli 1999) could have created an elevated thermal gradient; therefore, a value closer to 0.6  $\text{mm yr}^{-1}$  is considered to be appropriate. Cooling from 60 °C to surface temperature occurred in most of these samples within the time span of 18–10 Ma; this corresponds to bulk exhumation rates of ca. 0.2  $\text{mm yr}^{-1}$ . Significant changes in exhumation rates are not observed or were not within the resolution of our data.

Widespread Oligocene exhumation from the western Altiplano to the Eastern Cordillera most likely produced moderately elevated mountain ranges between which the

Altiplano Basin was filled. However, this surface uplift cannot be quantified.

Removal of Tertiary cover sediments and exposure of Palaeozoic rocks has increased erosional resistance since the Oligocene. Several indicators in the Eastern Cordillera south of ~18° S suggest that erosion rates decreased around ~15 Ma (see Horton (1999) for a summary) and, at this time, arid climatic conditions were established in the area west of the plateau (Alpers and Brimhall 1988; Sillitoe and McKee 1996).

Uplift was largely a function of tectonic shortening (cf. Isacks 1988), which continued after the end of internal deformation around 10 Ma due to underthrusting of the foreland (Allmendinger and Gubbels 1996; Kley et al. 1999). Probably, elevations along the eastern margin of the plateau became sufficiently high by 15–10 Ma to form a rain shadow, thus strongly decreasing erosional exhumation (Alpers and Brimhall 1988). However, paleo-geomorphological studies predict lower mean elevations of 1 000–1 500 m around 10 Ma (Kennan et al. 1997; Gregory-Wodzicki 2000; Kennan 2000).

The Tertiary sediments of the southern Altiplano were investigated in 10 localities south of the Salar de Uyuni (Fig. 13.2) and the stratigraphic columns, sedimentological features, and the results of isotope dating are depicted in Figs. 13.4 and 13.5, and Table 13.1.

A major change in basin configuration occurred with the onset of widespread, coarse-clastic sedimentation in the area of the present central Andean Plateau during the early Oligocene. This change is coeval with the onset of exhumational cooling at ca. 32 Ma (see above) within the plateau and was followed by the onset of volcanism at ~28 Ma. In contrast to the widespread playa-mudflat environments recorded in the Potoco Fm., the sedimentary characteristics of the overlying San Vicente Fm. indicate high relief, fault-bounded basins, and a coincidence between sedimentation, tectonism, and (since ~28 Ma) magmatism. The sedimentation forming the San Vicente Fm. probably began during the initial uplift of the plateau. A brief outline of the basin development implies four time intervals: Pre-32 Ma, 32–17 Ma, 17–8 Ma, and 8 Ma–Recent.

### 13.6 Sedimentary History of the Altiplano Basin and Adjacent Areas

In the southern Altiplano, an endorheic (internally-drained) basin was formed, presumably during the late Palaeocene, and persists today. Sediments and magmatic rocks, up to 8 km thick, were deposited and emplaced mainly during the Eocene to Miocene (Mertmann et al.

#### 13.6.1 Pre-32 Ma

The rocks underlying the Mesozoic to Cenozoic strata of the southern Altiplano Basin belong to different basement blocks. In the west, evidence for a shallow, but hidden, basement comes from pebbles within the Oligocene-Miocene San Vicente Fm. The clasts are mainly granites and gneisses of probable Precambrian age and Permian igneous rocks (Figs. 13.4 and 13.5, Table 13.1). Comparable

**Fig. 13.4.** Distribution of sample localities and age values for isotope age determinations (cf. Table 13.1). The map shows the western part of Fig. 13.2

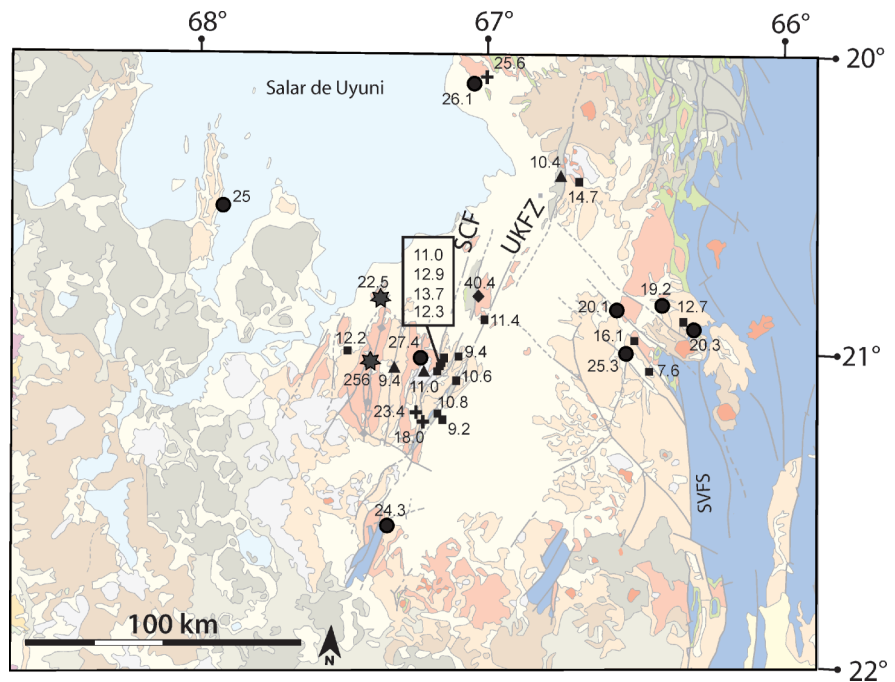


**Table 13.1.**  
K-Ar age data from the southern  
Altiplano

Sample	Age (Ma)	Mineral dated	Rock type	Position of sample	
				deg W	deg S
Flat-lying strata, unconformable over tilted San Vicente strata					
ED00-41	9.4 ±0.3	Biotite	Dacitic tuff	-67.3305	-21.0318
SR99-15	10.4 ±0.3	Biotite	Dacitic tuff	-66.7339	-20.3934
SR99-10	11.0 ±0.5	Hornblende	Andesitic lava	-67.2223	-21.0076
Upper San Vicente Formation, from growth strata					
ED 00-17	7.6 ±0.2	Biotite	Ignimbrite	-66.4193	-21.0481
ED 00-40	9.2 ±0.3	Biotite	Dacitic tuff	-67.1636	-21.1979
ED 00-07	9.4 ±0.3	Biotite	Dacitic tuff	-67.0998	-20.9969
ED 00-02	10.6 ±0.3	Biotite	Dacitic tuff	-67.1080	-21.0776
ED 00-33	10.8 ±0.3	Biotite	Dacitic tuff	-67.1657	-21.1940
PS 99/26	11.0 ±0.3	Biotite	Dacitic tuff	-67.1678	-21.0324
SR 99-06	11.4 ±0.3	Biotite	Dacitic tuff	-67.0085	-20.8749
ED 00-42	12.2 ±0.3	Biotite	Dacitic tuff	-67.4997	-20.9759
PS 99/47	12.3 ±0.4	Biotite	Dacitic tuff	-67.1437	-21.0288
ED 00-14	12.7 ±0.4	Biotite	Dacitic tuff	-66.2952	-20.8827
SR 99-13	12.9 ±0.3	Biotite	Dacitic tuff	-67.1755	-21.0376
PS 99/17	13.7 ±0.4	Biotite	Dacitic tuff	-67.1760	-21.0373
SR 99-01	14.7 ±0.4	Biotite	Dacitic tuff	-66.6676	-20.4152
DLP 02/2000	16.1 ±0.4	Biotite	Dacitic tuff	-66.4707	-20.9451
Lower San Vicente Formation					
ED 00-12	19.2 ±0.5	Biotite	Dacitic tuff	-66.3669	-20.8284
ED 00-10	20.1 ±0.5	Biotite	Dacitic tuff	-66.5333	-20.8427
PS 99/01	20.3 ±0.5	Biotite	Dacitic tuff	-66.2702	-20.8963
SR 99-14	24.3 ±1.2	Biotite	Andesitic tuff	-67.3566	-21.5611
SR 99-16	25.0 ±0.6	Biotite	Ignimbrite	-67.9466	-20.4903
AN 14/2000	25.3 ±1.0	Hornblende	Dacitic tuff	-66.4989	-20.9928
Chi 31/2000	26.1 ±0.7	Biotite	Dacitic tuff	-67.0334	-20.0702
SR 99-12	27.4 ±0.7	Biotite	Dacitic tuff	-67.2316	-21.0024
Intrusive rocks					
ED 00-31	18.0 ±0.5	Biotite	Granodiorite	-67.2372	-21.1956
ED 00-25	23.4 ±1.1	Hornblende	Diorite	-67.2407	-21.1933
ED 00-46	25.6 ±0.9	Hornblende	Andesite	-67.0220	-20.0640
Intrusive-derived clast from the lower San Vicente Formation					
ED 00-44	22.5 ±0.8	Hornblende	Microdiorite	-67.3783	-20.8015
ED 00-19	25.6 ±7	Hornblende	Granodiorite	-67.4194	-21.0144
Tuff from the Potoco Formation					
SR 99-03	40.4 ±1.1	Biotite	Dacitic tuff	-67.0295	-20.7959

rocks are exposed north of the Salar de Uyuni at Cerro Uyarani (Wörner et al. 2000). In the eastern part of the Altiplano, the basement is composed mainly of Ordovician to Devonian sedimentary rocks exposed along the UKFZ and in the Eastern Cordillera.

In the Altiplano, a significant angular unconformity is present between intensely foliated and folded Ordovician rocks and non-foliated late Ordovician (Cancaniri Fm.) and Silurian rocks. Cretaceous to Palaeocene rock se-

quences rest conformably on the Silurian strata. By contrast, in the Eastern Cordillera a marked angular unconformity of Carboniferous age (Müller et al. 2002) separates early Palaeozoic from Mesozoic and younger strata.

The Cretaceous to Palaeocene strata consist of terrigenous sediments, subordinate mafic volcanics and carbonates. In the early Cretaceous, deposition started in a small rift basin near Tupiza in the Eastern Cordillera. During the Maastrichtian and the Palaeocene, former ar-



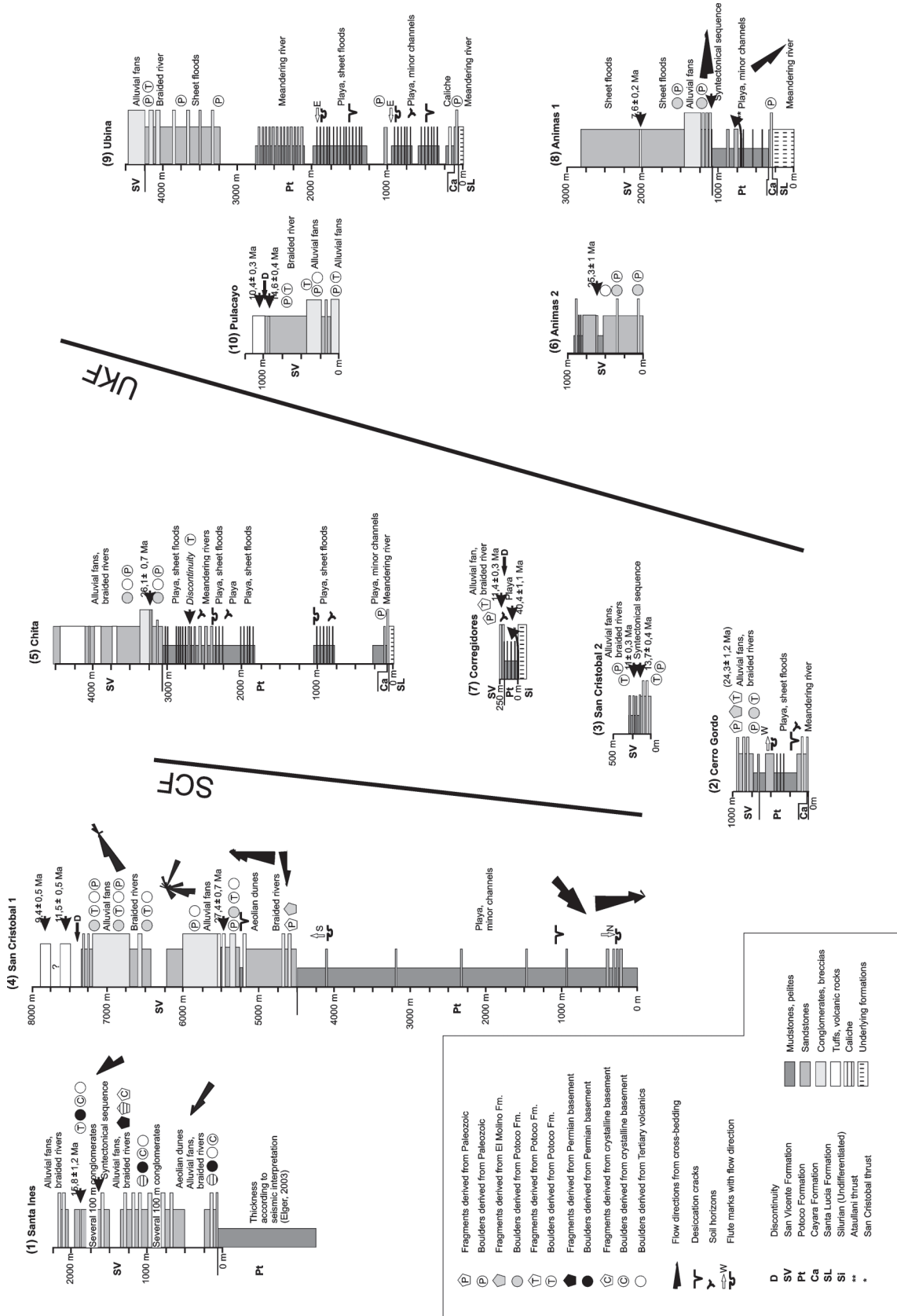


Fig. 13.5. Stratigraphic sections from the Altiplano with their respective position to major faults. For the location numbers and abbreviations refer to Fig. 13.2

eas of non-deposition were integrated into a post-rift basin extending from the Eastern Cordillera over the Altiplano to the Salar de Atacama region in Chile (Sempere 1995; Sempere et al. 1997, Fiedler 2001, Reutter et al. 2006, Chap. 14 of this volume). The limestones of the El Molino Formation and its equivalents are a significant, shallow marine, marker horizon indicating that the future plateau lay near sea level at the beginning of the Palaeocene. There are first indications of sediment transport from the central Eastern Cordillera towards the west, as well as to the east, (Horton and DeCelles 2001) in the Palaeocene-early Eocene Cayara Fm. (Silva-González 2004).

The Eocene Potoco Fm. shows significant differences between the eastern/central and the western Altiplano. To the east, an upwardly thickening and coarsening sequence (Lipez Basin, thickness > 3000 m) documents increasing relief along the eastern basin margin and shows a succession from the individual channels of a floodplain to a braided river environment. Flute casts and cross beds indicate an east to west transport direction (Fig. 13.5: Animas 1). To the west, the Potoco Fm. is mainly made up of red, thin-bedded to laminated pelites with frequent gypsum layers. The facies association points to deposition at the bottom of a quiet water column in a playa lake to playa-mudflat environment.

Provenance analyses of sandstones (Fig. 13.6) have revealed a predominantly recycled orogenic source, probably derived from the Palaeozoic basement of the Eastern Cordillera, but also, locally, a magmatic arc source which was situated in the Western Cordillera and in the Chilean Precordillera. In the western Altiplano, east-directed sediment transport has been reported by Almen-dras-Alarcón et al. (1997). Thus, we found evidence for the eastern as well as the western basin margins. This contrast with the findings of Horton et al. (2001) who described a persistent sediment source for the Potoco Formation only to the west associated with a paleocurrent reversal across the Santa Lucia–Potoco contact.

The Potoco Fm. is distributed throughout the Altiplano and, as revealed by seismic interpretations across the UKFZ, thicknesses vary significantly, probably owing to extensional tectonics (Elger 2003). The age of the Potoco Fm. is poorly constrained, however, a wind-blown tuff found near Corregidores provided an age of  $40.4 \pm 1.1$  Ma (K-Ar in biotite, Table 13.1, Fig. 13.4). This is in agreement with the palynomorph data published by Horton et al. (2001) from sections north of the Salar de Uyuni, which gave a late Eocene to Oligocene age for the majority of the Potoco strata. Horton et al. (2001) also inferred from age dating of the underlying Santa Lucia Fm. (~58 Ma, Sempere et al. 1997) that the lowermost Potoco Fm. was deposited during the late Palaeocene to middle Eocene. In general, the sedimentary characteristics of the Potoco Fm. indicate a relatively low relief (except for the eastern basin margin) and little tectonic activity.

### 13.6.2 The Early Oligocene Turnover and the 32–17 Ma Interval

In the center of the Altiplano Basin, the Potoco Fm. is overlain by the San Vicente Fm. which spans an age interval of about 32–10 Ma. The boundary between both formations is marked by the first appearance of breccias and conglomerates containing Palaeozoic clasts. The contact between the two formations is conformable west of the San Cristobal fault, which is the westernmost branch of the UKFZ (SCF in Figs. 13.2 and 13.3), but angular unconformities have been observed towards the east. Moreover, in several localities the San Vicente Fm. directly rests on Silurian or Ordovician strata along the UKFZ, indicating a considerable erosional phase prior to its deposition and a strong palaeo-relief. For example, in the Cerro Gordo area, the San Vicente Fm. lies on foliated Ordovician strata. Basal tuffs are  $24.3 \pm 1.2$  Ma old, indicating

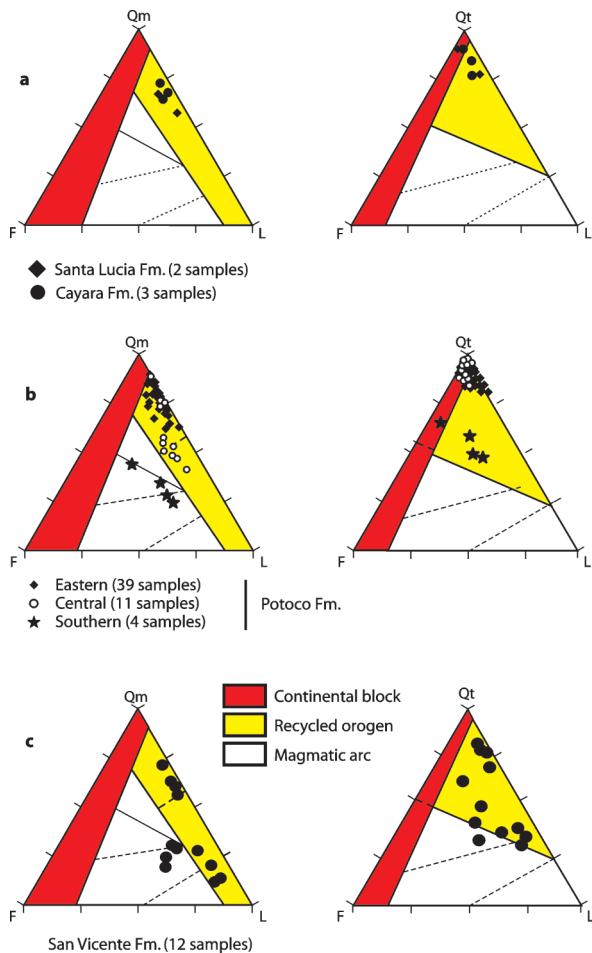


**Fig. 13.6.** Provenance of sandstones from the Altiplano according to Dickinson and Suczek (1979). **a** Palaeocene (Cayara and Santa Lucia Fms.); **b** Eocene (Potoco Fm.); **c** Oligocene-Miocene (San Vicente Fm.). Qm: monocrystalline quartz; Qt: total quartz; F: feldspar; L: lithics

that this phase of erosion had taken place in the late Oligocene or earlier.

The age of basal San Vicente sediments varies considerably. West of the UKFZ, deposition started in the early Oligocene, but east of it, sedimentation began in the late Oligocene to early Miocene (between 20 and 25 Ma). In the San Cristobal section, a complete profile of the Potoco and San Vicente deposits has been investigated. Here, the first volcanic intercalations (K-Ar in biotite:  $27.4 \pm 0.7$  Ma) have been found some 900 m above the base of this ~4000 m thick formation, but, owing to the presence of volcanic boulders in the conglomerates 750 m above the base, the onset of volcanism should have occurred somewhat earlier.

To estimate when deposition of the San Vicente Fm. began, we tentatively assumed a constant sedimentation rate for the entire formation, thus implying an age of ~32 Ma for the base of the San Vicente strata. This is significantly earlier than the onset of volcanism. The first occurrence of Palaeozoic clasts in the basal San Vicente would then be coeval with the onset of exhumational cooling (33–29 Ma) along the UKFZ to the east (see above). In the Chita section (Fig. 13.5), where the San Vicente Fm. also lies conformably upon Potoco strata, the basal San Vicente conglomerates contain volcanic clasts, besides Palaeozoic and El Molino (late Cretaceous – Palaeocene) clasts. An age of  $26.1 \pm 0.7$  Ma was derived from the lowermost tuff, approximately 200 m above the base.

The San Vicente Fm. differs considerably from the Potoco Fm. It is composed of breccias, conglomerates, sandstones (Fig. 13.5), pelites, tuffaceous sandstones, tuffs and lavas in a complicated lateral and vertical facies amalgamation. Thickness varies considerably within the basin, reaching a maximum of ca. 4000 m west of the UKFZ in the San Cristobal area. Towards the west and the south, thicknesses diminish gradationally, whereas to the east, across the UKFZ, there is a remarkable change in the San Vicente thickness from these maximum values to only several tens of meters.

Facies associations of the San Vicente Fm. comprise alluvial fans, aeolian deposits, fluvial systems, and subordinate lacustrine and playa associations (Mertmann et al. 2003). Conglomerates and breccias of the western Altiplano region are derived from a granitic and metamorphic basement of probable Precambrian age, as well as from Permian volcanics that were exhumed around 28 Ma (see above).

Detrital AFT cooling ages of these components record rapid exhumation from ~32 Ma in the western source areas. In the central and eastern parts, all sections show a predominance of clasts derived from the early Palaeozoic sedimentary basement mixed with minor amounts of clasts derived from the Potoco Fm. and the late Cretaceous – Palaeocene El Molino Fm. It is important to note that in the vicinity of the SCE, the basal San Vicente Fm. consists of breccias containing Palaeozoic and El Molino clasts indicating the existence of nearby basement highs

when deposition of the San Vicente Fm. began. The same clast compositions exist in Cerro Gordo as well as breccia horizons which, however, also contain Potoco clasts.

Volcanic rocks, tuffs and lahar suites indicate intense volcanism during much of the late Oligocene to Miocene. This corresponds to the magmatic arc source indicated by the provenance analyses diagrams of the San Vicente Fm. (Fig. 13.6).

### 13.6.3 17–8 Ma (Miocene)

In the upper part of the San Vicente Fm. (Pilkhausa subsequence, Elger 2003), growth strata are developed along thrusts indicating deposition during shortening deformation. The age data from the upper part of the San Vicente Fm. range between 16.1 and 7.6 Ma (Table 13.1). Synthrusting sequences with progressive unconformities have been observed in the Pulacayo, Santa Ines, Animas 1, and San Cristobal sections. The alluvial fans and fluvial systems are composed once more of conglomerates and sandstones, tuffaceous sandstones, tuffs and lavas. In younger parts of the San Vicente Fm., Potoco-derived clasts clearly become more frequent than in the lower part, indicating a significant change in the composition of the source area. The overall tendency of the associated sediment is an upwardly coarsening cycle, which may point to a thrust source (see below). Exhumation in the hanging wall of the San Cristobal fault started around 20 Ma. Hence, the thick strata of the former half-graben were thrust to the east, tilted, and eroded, plausibly explaining these significant sedimentological changes in the upper San Vicente. The San Vicente strata are overlain by late Miocene volcanics and volcanoclastic sediments with an angular unconformity. The age of the unconformity varies between approximately 11 and 8 Ma (Table 13.1).

### 13.6.4 8 Ma – Recent

After the late Miocene deformation events, the southern Altiplano remained an endorheic basin developing during a tectonic quiescence that has characterized both the Altiplano and the Eastern Cordillera over the last 8 million years. Strata younger than 8 Ma are flat-lying, and no significant faults have been observed. Undeformed sediments covering the San Juan del Oro peneplain are distributed over SW Bolivia and the Puna of NW Argentina (Müller et al. 2002). Our AFT results suggest that the inner part of the foreland-thrust belt (Interandean zone) had largely formed by this time, and that the eastern deformation front stepped into the Subandean zone. The zone of active shortening and uplift is located approximately 10 to 20 km east of the easternmost frontal range of the Subandean belt, below the Chaco plain.

The sedimentary sequences of the Interandean, Subandean and Chaco area document the eastward migration of the Andean orogenic front. This can be shown by the development of the foreland basin infill of the Chaco Basin. This infill can be subdivided into five formations: the *Petaca*, *Yecua*, *Tariquia*, *Guandacay* and *Emborozu* (Hulka et al. in press, Uba et al. in press).

The *Petaca Fm.* (approximately 60 to 15 Ma, Marshall and Sempere 1991; Marshall et al. 1993) is up to 50 m thick and consists of duricrusts interbedded with channel fills of poorly-defined, sandy, ephemeral streams deposited in an arid, braidplain environment. During the mid to late Miocene, several short-lived, weak, marine transgressions occurred and the marine lagoonal to tidal facies of the *Yecua Fm.* may represent the underfilled stage and distal position of the eastward-advancing, Andean foredeep. The *Yecua Fm.* is overlain by fluvial redbeds, up to 2 km thick, of the *Tariquia Fm.* The provenance of this formation is from the west; the medium-grained, multiply-recycled quartz grains clearly record the uplift and unroofing of major continental sedimentary sequences to the west.

The base of the overlying *Guandacay Fm.* (Miocene – Pliocene, more than 100 m thick) is conventionally drawn at the first sustained occurrence of pebble conglomerates. The contact is gradational and marks the passing from lowland, anastomosing streams and semiarid floodplains to gravelly, braided fluvial systems, and suggests an approaching source area of high relief. The base of the youngest unit of the Chaco Basin fill, the *Emborozu Fm.* (Pliocene – Pleistocene), is marked by the first sustained occurrence of cobble and boulder conglomerates. These mark alluvial fan facies and the proximity of high morphological relief. The *Guandacay* and *Emborozu Fms.* are almost exclusively exposed near the present mountain front and grade eastwards, presumably rapidly, into finer-grained deposits, overlain by the Quaternary floodplain and aeolian deposits of the Chaco plain. As stated above, the Miocene to Pleistocene sedimentary sequences of the Chaco indicate the approach of the Andean thrust front, which is also reflected in the AFT data.

### 13.7 Discussion

Our sedimentary and exhumational data have tectonic implications for plateau evolution and, furthermore, are relevant to the evolution of the Andean active margin. Our results show four stages in the tectonic evolution of the southern Altiplano plateau and adjacent areas:

1. *Pre 32 Ma*: Relative tectonic quiescence in the Altiplano Basin, Incaic shortening in the Precordillera (45–38 Ma) and initial thrusting and uplift in the Proto Eastern Cordillera (40–36 Ma).
2. *32–17 Ma*: Exhumation, creation of strong relief, construction of a magmatic arc (from ~28 Ma). Deformation restricted to the present plateau, extension in the Altiplano, shortening in the Eastern (and Western) Cordillera.
3. *17–8 Ma*: Shortening in the entire plateau, beginning of thrusting onto the foreland.
4. *8–0 Ma*: Shortening in the foreland, tectonic quiescence in the plateau.

#### 13.7.1 Tectonic Implications of the Sedimentary and Exhumational Result

The Andean high plateau and adjacent areas are characterized by surface uplift and exhumation, as well as by strong subsidence of sedimentary basins since the Palaeogene. In areas, exhumed along major faults, the Palaeozoic and Precambrian basement is eroded, whereas basinal areas receive continental detritus, in some places up to 8 km thick (Oligo-Miocene San Vicente Fm.: 4 km). Today, these basins are thrust-bound. However, the observations of Elger (2003) indicate that normal faulting has also played an important role during the basin evolution in the Altiplano. Our AFT data show that inversion of normal faults occurred around 17 Ma, during deposition of the San Vicente Fm. (see below). This inversion contrasts with the evolution of the Eastern Cordillera where, according to Müller et al. (2002), shortening has prevailed since the late Eocene.

At the beginning of the Tertiary and before ~32 Ma, the Altiplano was near sea level, evidenced by the marine strata of the El Molino Fm. (Sempere et al. 1997). This does not seem to have changed fundamentally until the early Oligocene. In the central Eastern Cordillera, however, exhumation started in the late Eocene (see above and cf. Lamb and Hoke 1997). Sandstone composition and the upward coarsening of sediment in the Potoco Fm., shed from the Proto-Cordillera, indicate growing relief at the basin margin. The thicknesses of Potoco sediments vary strongly from some hundred meters to (locally) 4000 m.

In general, sedimentary thicknesses can be attributed to some crustal thickening and, thus, some uplift. On the other hand, Potoco extension of about 5% (Elger 2003) caused crustal thinning. A quantitative estimate of these concurring processes is difficult since the original thickness of the Potoco Fm. is known only from a few conformable successions into the San Vicente Fm. It seems, however, that there was only little uplift in the central Altiplano before the early Oligocene. This concurs with the uplift history data of Gregory-Wodzicki (2000) which state no uplift before the early Miocene.

With the beginning of San Vicente deposition, a major change in basin configuration took place. Differential uplift produced local basement highs where Cretaceous

and Palaeozoic units became exposed. The distribution of sediments, for example, across the west-dipping SCF is such that to the east, i.e. in the footwall of this fault, thicknesses of the Potoco and San Vicente Fms. are only 400 m and 200 m, respectively (Elger 2003; Silva-González 2004). West of the fault, each formation reaches a maximum thickness of 4000 m. This indicates that the basement high was already bounded by a precursor to the San Cristobal fault.

Questions arise about the kinematic regime of this precursor fault during early San Vicente time. We suggest that the variations in sedimentary thickness across the SCF is more indicative of normal faulting than of thrusting, although, today, this steeply westward-dipping fault shows thrusting kinematics which, according to the AFT data, took place in the mid to late Miocene (20–11 Ma). If these expansive thicknesses were accommodated in the back of a thrust fault, this would imply an exceptionally thick, piggyback basin fill on top of the thrust strata, in contrast to a very thin foreland infill.

Furthermore, if this maximum thickness of 4000 m was accommodated behind the thrust, the components should represent an inverse lithostratigraphical succession. This, however, contrasts with the spectrum of components in the San Vicente Fm., which predominantly contains Palaeozoic clasts from the base upward. The Palaeozoic components of this formation are only poorly rounded indicating the existence of a nearby source area at approximately 32 Ma. East-west extension is also in accordance with the orientation of N-S-trending mafic dikes ( $25.6 \pm 0.9$  Ma) that have been found in the Chita area.

To the west, the San Vicente Basin was bounded by a basement high composed of Proterozoic to Permian rocks, representing the western source area of the Tertiary strata. However, due to poor outcrop data we cannot decide whether the San Vicente depocenter was a half-graben or graben setting. The seismic interpretations of Elger (2003) rather indicate a half-graben setting.

Since ca. 28 Ma, widespread volcanic activity created further relief and an additional source of sediment supply. West of the UKFZ, the depocenter persisted and formed a local intra-arc basin, probably still bounded by a normal fault. This extensional basin was inverted, but the onset of contraction is poorly constrained. Exhumation of the depocenter west of the San Cristobal fault yields a minimum age of 20 Ma. Clearly, the major phase of shortening in the central Altiplano began by 20–19 Ma (Elger 2003).

### 13.7.2 Interpretation in the Context of the Andean Active Continental Margin Evolution

Before 38 Ma, the Altiplano occupied a back-arc position in relation to the magmatic arc in the Chilean Precordil-

lera (Fig. 13.7a; Charrier and Reutter 1994). At the beginning of the Palaeogene, this back-arc area formed one single basin and the generally fine-grained sediments in the basin center seem to indicate weak relief. However, the original basin progressively divided into smaller basins owing to the uplift of the central Eastern Cordillera (Protocordillera, Lamb and Hoke 1997), which became the source area for fringing river systems.

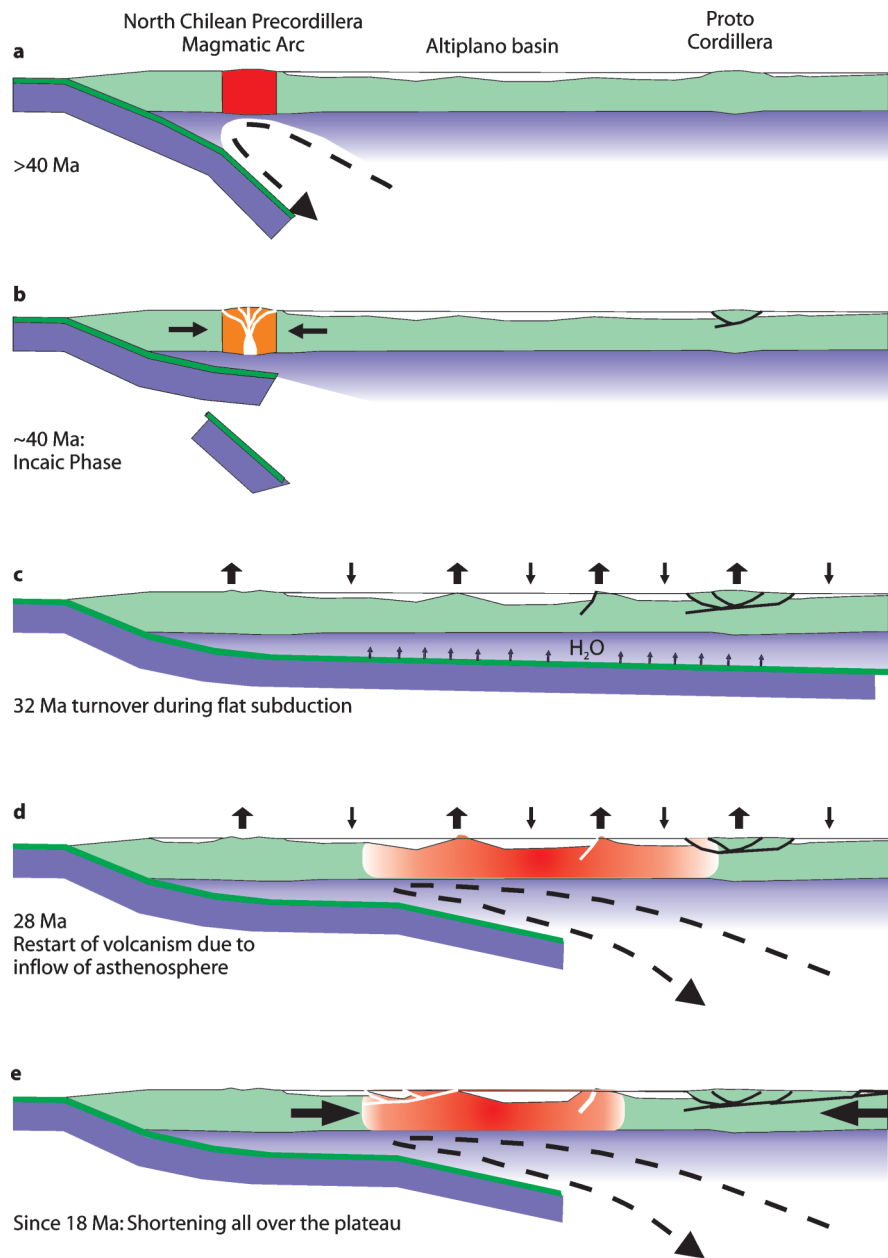
During this time, internal normal faults might have been active (Elger 2003), thus already indicating areas of, later accentuated, tectonic basin segmentation. AFT data indicate that uplift occurred in the central Eastern Cordillera caused by initial thrusting increments between 40 and 36 Ma (Fig. 13.7b). These thrusting movements partly overlapped with the Incaic phase transpressional movements that affected the magmatic arc in the north Chilean Precordillera between 45 and 38 Ma (Haschke and Günther 2003). Thus, there were deformations in two zones separated by an approximately 430 km wide zone of tectonic quiescence and some normal faulting.

Around 38 Ma, volcanism ceased in the Chilean Precordillera for some 10 million years (Döbel et al. 1992). This period was crucial for the early evolution of the central Andean Plateau: Exhumational cooling started around 32 Ma along discrete faults (Fig. 13.7c) distributed between the eastern margin of the Eastern Cordillera and the western Altiplano, and possibly continued into the north Chilean Precordillera (Maksaev and Zentilli 1999), i.e. over the future plateau area which was > 400 km wide before the onset of Andean shortening. Exhumation occurred together with a fundamental change in the sedimentary record in adjacent basins prior to the resumption of volcanism at ~28 Ma, as the first (and oldest) volcanic intercalations in the San Vicente Fm. have been found 900 m above its base.

Our ages for the described tectonic events of between 38 and 32 Ma is in good agreement with Gephart's (1994) age for the initial uplift of the central Andean Plateau. Gephart considered topographic and slab symmetry and suggested the beginning of plateau formation at about 35 Ma. Given the uncertainties in age dating, this seems a rather good accordance.

A clue for understanding this early plateau comes from inferences about the subduction geometry in the early Oligocene when the downgoing slab was probably nearly horizontal at 100 km depth (James and Sacks 1999; Haschke et al. 2002, Reutter 2001). This so-called flat subduction probably was caused by slab detachment which has been suggested by Fukao et al. (2001) to have occurred in the circum-Pacific subduction zones in the Eocene epoch. Flat subduction has severe consequences for the tectonic regime in the upper plate. According to Gutscher et al. (2000), flat subduction leads to a pause in volcanism and to strong intraplate coupling, which leads to strong deformation in the cold seismogenic crust of the

**Fig. 13.7.** Cartoons showing the tectonic evolution of the central Andean Plateau around 21° S



upper plate. Deformation is concentrated on the zone above the point where the slab resteepestens, and this could explain how shortening deformation jumped from the north Chilean Precordillera to the Eastern Cordillera.

A further consequence of flat subduction should be the hydration of the upper plate mantle. The water carried by the subducting slab might have migrated into the upper plate mantle, partially altering the mantle peridotite into serpentinite. Serpentinization, in turn, increased the volume of the mantle by decreasing its density, consequently making a considerable contribution to the initial uplift of the future plateau. The inferred extensional

movements might be caused by variations in the degree of coupling between the plates from the central Altiplano to the Eastern Cordillera. They might also be due to local and near-surface effects of differential uplift, perhaps owing to variations in the degree of hydration in the lithospheric mantle.

Around 28 Ma, subsequent to the beginning of exhumation and faulting, magmatism started again in the Central Andes over a very wide area, reaching from the Western Cordillera over the Altiplano to the Eastern Cordillera (Fig. 13.7d). Intense and widespread magmatic activity, which is strongly reflected in the composition of

sandstones (Fig. 13.6), began with basaltic-andesitic to silicic lavas, tuffs, and shallow intrusions. The southern Altiplano also became part of the Central Andean magmatic arc. Such a broad arc indicates a rather low dip angle for the subducting slab, which, however, must have been steep enough to allow the formation of an asthenospheric wedge (Tatsumi and Eggins 1995). Thus, since the restart of volcanism, uplift should have been accompanied by lithospheric thinning together with crustal thickening because of distributed shortening within the plateau, as has been suggested by Isacks (1988).

Around 18 Ma, shortening started in the Altiplano (Fig. 13.7e), and the Andean orogen was progressively thrust along the Interandean thrust onto the Brazilian shield (Jordan et al. 1997). Thus, crustal thickening has been the major plateau-forming process since that time. A further change occurred in the Andean system around 10 Ma. Before this time, shortening occurred in the plateau and in the western foreland, but after 10 Ma, deformation ceased in the plateau (Gubbels et al. 1993), becoming stronger in the foreland. The termination of deformation within the plateau was accompanied by the underthrusting of cold Brazilian shield lithosphere, causing a narrowing of the magmatic arc and restricting it to the Western Cordillera. The Altiplano and the Eastern Cordillera are now underlain by a cold thick lithosphere mantle (Whitman et al. 1992).

To conclude, the style of deformation changed through the stages outlined above: shortening and extension operated simultaneously during initial plateau formation (32–19 Ma); between 19 and 8 Ma, shortening occurred within the plateau and also in the eastern foreland; and since 8 Ma, shortening has been localized to the thin-skinned fold-and-thrust belt in the eastern foreland. Furthermore, uplift during the first two stages occurred together with subsidence over wide parts of the plateau. Neither a migration of an exhumation front nor an eastward propagation of a thrust front operated before 18 Ma. A further important result is that initial plateau formation occurred significantly earlier than the onset of volcanism.

## Acknowledgments

Research was supported by the Deutsche Forschungsgemeinschaft and the Freie Universität Berlin (Sonderforschungsbereich 267 “Deformation Processes in the Andes”). We thank O. Oncken for helpful discussions. Fieldwork was facilitated by Umberto Castro, Reinhard Rössling and Heriberto Salamanca. The manuscript was improved by the constructive reviews of Teresa Jordan, (Cornell University, Ithaca New York) and Fritz Schlunegger (University of Bern).

## References

- Allmendinger RW, Gubbels T (1996) Pure and simple shear plateau uplift, Altiplano-Puna, Argentina and Bolivia. *Tectonophysics* 259: 1–14
- Almendras-Alarcón OD, Baldelón EG, López R (1997) Hoja geológica Volcán Ollague/San Agustín. Programa Carta Geológica de Bolivia 1: 100 000, Publ. SGM Serie I-CGB-46 SG
- Alpers CN, Brimhall GH (1988) Middle Miocene climatic change in the Atacama Desert, northern Chile: evidence from supergene mineralization at La Escondida. *Geol Soc Am Bull* 100:1640–1656
- Andriessen PAM, Reutter K-J (1994) K-Ar and fission track mineral age determinations of igneous rocks related to multiple magmatic arc systems along the 23°S latitude of Chile and NW Argentina. In: Reutter K-J, Scheuber E, Wigger P (eds) *Tectonics of the Southern Central Andes*. Springer-Verlag, Berlin Heidelberg New York, pp 141–153
- Babayko AY, Sobolev SV, Trumbull RB, Oncken O, Lavier LL (2002) Numerical models of crustal scale convection and partial melting beneath the Altiplano-Puna plateau. *Earth Planet Sci Lett* 199: 373–388
- Baby P, Herail H, Salinas R, Sempere T (1992) Geometry and kinematic evolution of passive roof duplexes deduced from cross-section balancing: Example from the foreland thrust system of the southern Bolivian Subandean Zone. *Tectonics* 11:523–536
- Baby P, Rochat P, Herail G, Mascle P, Paul A (1996) Neogene thrust geometry and crustal balancing in the northern and southern branches of the Bolivian orocline (Central Andes). *International Symposium on Andean Geodynamics 3*, Saint Malo
- Baby P, Rochat P, Herail H, Mascle G (1997) Neogene shortening contribution to crustal thickening in the back arc of the Central Andes. *Geology* 25:883–886
- Bahlburg H, Breitzkreuz C, Zeil W (1986) Paläozoische Sedimente Nordchiles. *Berliner Geowiss Abh* A66, pp 147–168
- Benjamin MT, Johnson NM, Naeser CW (1987) Recent rapid uplift in the Bolivian Andes: evidence from fission-track dating. *Geology* 15:680–683
- Brown RW, Summerfield MA (1997) Some uncertainties in the derivation of rates of denudation from thermochronologic data. *Earth Surf Process Landforms* 22:239–248
- Carlson WD, Donelick RA, Ketcham RA (1999) Variability of apatite fission-track annealing kinetics: I. Experimental results. *Am Mineralogist* 84:1213–1223
- ChARRIER R, Reutter K-J (1994) The Purilactis Group of Northern Chile: boundary between arc and backarc from late Cretaceous to Eocene. In: Reutter K-J, Scheuber E and Wigger P (eds) *Tectonics of the Southern Central Andes*. Springer-Verlag, Berlin Heidelberg New York, pp 189–202
- DeCelles PG, Horton BK (2003) Early to middle Tertiary foreland basin development and the history of Andean crustal shortening in Bolivia. *Geol Soc Am Bull* 115:58–77
- Dickinson WR, Suczek CA (1979) Plate tectonics and sandstone compositions. *Am Ass Petrol Geol Bull* 63:2164–2182
- Döbel R, Friedrichsen H, Hammerschmidt K (1992) Implication of  $^{40}\text{Ar}/^{39}\text{Ar}$  dating of early Tertiary volcanic rocks from the North Chilean Precordillera. *Tectonophysics* 202:55–81
- Dunn JF, Hartshorn KG, Hartshorn PW (1995) Structural styles and hydrocarbon potential of the Subandean Belt of southern Bolivia. In: Tankard AJ, Suarez R, Welsink HJ (eds) *South American Petroleum Basins*. AAPG Memoir 62, pp 523–543
- Ege H (2004) Exhumations- und Hebungsgeschichte der zentralen Anden in Südbolivien (21°S) durch Spaltspur-Thermochronologie an Apatit. PhD thesis, Freie Universität Berlin

- Ege H, Sobel E, Jacobshagen V, Scheuber E, Mertmann D (2003) Exhumation history of the Central Andes of southern Bolivia by apatite fission track dating. *Revista Tecnica YPFB* 21:165–172
- Ege H, Sobel ER, Scheuber E, Jacobshagen V (submitted) Exhumation history of the Central Andean plateau (southern Bolivia) constrained by apatite fission track thermochronology. Submitted to *Tectonics*
- Elger K (2003) Analysis of deformation and tectonic history of the Southern Altiplano Plateau (Bolivia) and their importance for plateau formation. *GeoForschungsZentrum Potsdam, Scientific technical report STR 03/05*, pp 1–152
- Elger K, Oncken O, Glodny J (2005) Plateau-style accumulation of deformation – the Southern Altiplano. *Tectonics* (in press)
- Fiedler K (2001) Die kretazisch-alttertiäre Entwicklung des südlichen Potosí-Beckens (Süd-Bolivien). *Berliner Geowiss Abh A215*:1–185
- Fiedler K, Mertmann D, Jacobshagen V (2003) Cretaceous marine incursions in the southern Potosi basin of southern Bolivia: tectonic and eustatic control. *Revista Tecnica YPFB* 21:157–164
- Fitzgerald PG, Sorkhabi RB, Redfield TF, Stump E (1995) Uplift and denudation of the central Alaska Range: a case study in the use of apatite fission track thermochronology to determine absolute uplift parameters. *J Geophys Res* 100:20175–20191
- Fukao Y, Widiyantoro S, Obayashi M (2001) Stagnant slabs in the upper and lower mantle transition region. *Rev Geophys* 39(3): 291–323
- Gallagher K (1995) Evolving temperature histories from apatite fission-track data. *Earth Planet Sci Lett* 136:421–435
- Gephart JW (1994) Topography and subduction geometry in the central Andes: clues to mechanics of a noncollisional orogen. *J Geophys Res* 99(B6):12279–12288
- Green PF, Duddy IR, Laslett GM, Hegarty KA, Gleadow AJW, Lovering JF (1989) Thermal annealing of fission tracks in apatite. 4. Quantitative modelling techniques and extension to geological time-scales. *Chem Geol (Isotope Geosci Sec)* 79:155–182
- Gregory-Wodzicki KM (2000) Uplift history of the Central and Northern Andes: a review. *Geol Soc Am Bull* 112(7):1091–1105
- Gubbels TL, Isacks BL, Farrar E (1993) High-level surfaces, plateau uplift, and foreland development, Bolivian central Andes. *Geology* 21:695–698
- Günther A (2001) Strukturgeometrie, Kinematik und Deformationsgeschichte des oberkretazisch-alttertiären magmatischen Bogens (nord-chilenische Präkordillere, 21.7°–23°S). *Berliner Geowiss Abh A* 213
- Gutscher ME, Spakman W, Bijwaard H, Engdahl ER (2000) Geodynamics of flat subduction: seismicity and tomographic constraints from the Andean margin. *Tectonics* 19(5):814–833
- Hansen DL, Nielsen SB (2003) Why rifts invert in compression. *Tectonophysics* 373:5–24
- Haschke M, Günther A (2003) Balancing crustal thickening in arcs by tectonic vs. magmatic means. *Geology* 31(11):933–936
- Haschke M, Scheuber E, Günther A, Reutter K-J (2002) Evolutionary cycles during the Andean orogeny. repeated slab breakoff and flat subduction? *Terra Nova* 14(1):49–55
- Henry SG, Pollack HN (1988) Terrestrial heat flow above the Andean subduction zone in Bolivia and Peru. *J Geophys Res* 93: 15153–15162
- Hindle D, Kley J, Klosko E, Stein S, Dixon T, Norabuena E (2002) Consistency of geologic and geodetic displacements in Andean orogenesis. *Geophys Res Lett* 29: doi 10.1029/2001GL013757
- Hindle D, Kley J, Oncken O, Sobolev S (2005) Crustal flux and crustal balance from shortening estimates in the Central Andes. *Earth Planet Sci Lett* 230:113–124
- Horton BK (1998) Sediment accumulation on top of the Andean orogenic wedge: Oligocene to Late Miocene basins of the Eastern Cordillera, Southern Bolivia. *Geol Soc Am Bull*, 110(9):1174–1192
- Horton BK (1999) Erosional control on the geometry and kinematics of thrust belt development in the central Andes. *Tectonics* 18:1292–1304
- Horton BK, DeCelles PG (2001) Modern and ancient fluvial megafans in the foreland basin systems of the central Andes, southern Bolivia: implications for drainage network evolution fold-thrust belts. *Basin Research* 13:43–63
- Horton BK, Hampton BA, Waanders GL (2001) Paleogene synorogenic sedimentation in the Altiplano plateau and implications for initial mountain building in the central Andes. *Geol Soc Am Bull* 113(11):1387–1400
- Hulka C, Gräfe K-U, Sames B, Uba CE, Heubeck C (in press) Depositional setting of the middle to late Miocene Yecua Formation of the Chaco foreland basin, southern Bolivia. *J S Am Earth Sci*
- Isacks BL (1988) Uplift of the Central Andean Plateau and bending of the Bolivian Orocline. *J Geophys Res* 93:3211–3231
- James DE, Sacks IS (1999) Cenozoic formation of the Central Andes: a geophysical perspective. In: Skinner BJ (ed) *Geology and ore deposits of the Central Andes*. *Spec Pub Soc Econ Geol* 7, pp 1–25
- Jordan TE, Reynold JH III, Erikson JP (1997) Variability in age of initial shortening and uplift in the Central Andes, 16–33°30'S. In: Ruddiman WF (ed) *Tectonic uplift and climate change*. Plenum Press, pp 41–61
- Kennan L (2000) Large-scale geomorphology of the Andes: interrelationships of tectonics, magmatism and climate. In: Summerfield MA (ed) *Geomorphology and global tectonics*. John Wiley & Sons, Chichester, pp 167–200
- Kennan L, Lamb SH, Hoke L (1997) High altitude palaeosurfaces in the Bolivian Andes: evidence for late Cenozoic surface uplift. In: Widdowson M (ed) *Palaeosurfaces: recognition, reconstruction and interpretation*. *Geol Soc London Spec Pub* 120, pp 307–324
- Ketcham RA, Donelick RA, Carlson WD (1999) Variability of apatite fission-track annealing kinetics: III. Extrapolation to geological time scales. *Am Mineralogist* 84(9):1235–1255
- Ketcham RA, Donelick RA, Donelick MB (2000) AFT-Solve: a program for multi-kinetic modeling of apatite fission-track data. *Geol Materials Res* 2(1):1–32
- Kley J (1996) Transition from basement-involved to thin-skinned thrusting in the Cordillera Oriental of southern Bolivia. *Tectonics* 15:763–775
- Kley J, Müller J, Tawackoli S, Jacobshagen V, Manutsoglu E (1997) Pre-Andean and Andean-age deformation in the Eastern Cordillera of Southern Bolivia. *J S Am Earth Sci* 10(1):1–19
- Kley J, Monaldi CR, Salfity JA (1999) Along-strike segmentation of the Andean foreland: causes and consequences. *Tectonophysics* 301:75–94
- Kontak DJ, Farrar E, Clark AH, Archibald DA (1990) Eocene tectonothermal rejuvenation of an upper Palaeozoic-lower Mesozoic terrane in the Cordillera de Carabaya, Puno, southeastern Peru, revealed by K-Ar and <sup>40</sup>Ar/<sup>39</sup>Ar dating. *J S Am Earth Sci* 3(4):231–246
- Lamb S (2000) Active deformation in the Bolivian Andes, South America. *J Geophys Res* 105(11):25627–25653
- Lamb S, Hoke L (1997) Origin of the high plateau in the Central Andes, Bolivia, South America. *Tectonics* 16:623–649
- Lamb S, Hoke L, Kennan L, Dewey J (1997) Cenozoic evolution of the Central Andes in Bolivia and northern Chile. In: Burg JP, Ford M (eds) *Orogeny through time*. *Geol Soc Spec Pub* 121, pp 237–264
- Maksaev V, Zentilli M (1999) Fission track thermochronology of the Domeyko Cordillera, northern Chile: implications for Andean tectonics and porphyry copper metallogenesis. *Expl Mining Geol* 8:65–89
- Marquillas RA, Salfity JA (1994) Tectonic and sedimentary evolution of the Cretaceous-Eocene Salta Group, Argentina. In: Salfity JA (ed) *Cretaceous Tectonics of the Andes*. *Earth Evolution Science* 6, pp 266–315



- Marshall LG, Sempere T (1991) The Eocene to Pleistocene vertebrates of Bolivia and their stratigraphic context: a review. In: Suarez-Soruco R (ed) *Vertebrados*. Revista técnica de YPPFB 12, pp 631–652
- Marshall LG, Sempere T, Gayet M (1993) The Petaca (Late Oligocene–Middle Miocene) and Yecua (Late Miocene) formations of the Subandean-Chaco basin Bolivia and their tectonic significances. Documents du laboratoire de Lyon, pp 291–301
- Mertmann D, Scheuber E, Silva-González P, Reutter K-J (2003) Tectono-sedimentary evolution of the southern Altiplano: basin evolution, thermochronology and structural geology. *Revista técnica de YPPFB*, 21: 17–22
- Moretti I, Baby P, Mendez E, Zubieta D (1996) Hydrocarbon generation in relation to thrusting in the Subandean zone from 18° to 22°S, South Bolivia. *Petrol Geosci* 2:17–28
- Müller J (2000) Tektonische Entwicklung und Krustenverkürzung der Ostkordillere Südbolivians (20.7°S–21. 5°S). PhD thesis, Freie Universität Berlin
- Müller JP, Kley J, Jacobshagen V (2002) Structure and Cenozoic kinematics of the Eastern Cordillera, southern Bolivia (21°S). *Tectonics* 21: doi 10.1029/2001TC001340
- Reutter K-J (2001) Le Ande centrali: elementi di un' orogenesi di margine continentale attivo. *Acta Naturalia de "L' Ateneo Parmense"* 37(1/2):5–37
- Reutter K-J, Charrier R, Götze H-J, Schurr B, Wigger P, Scheuber E, Giese P, Reuther C-D, Schmidt S, Rietbrock A, Chong G, Belmonte-Pool A (2006) The Salar de Atacama Basin: a subsiding block within the western edge of the Altiplano-Puna Plateau. In: Oncken O, Chong G, Franz G, Giese P, Götze H-J, Ramos VA, Strecker MR, Wigger P (eds) *The Andes – active subduction orogeny*. *Frontiers in Earth Science Series*, Vol 1. Springer-Verlag, Berlin Heidelberg New York, pp 303–326, this volume
- Sempere T (1994) Kimmeridgian to Paleocene tectonic evolution of Bolivia. In: Salfity JA (ed) *Cretaceous Tectonics in the Andes*. *Earth Evolution Science* 6, pp 169–212
- Sempere T (1995) Phanerozoic evolution of Bolivia and adjacent regions. In: Tankard AJ, Suárez SR, Welsink, HJ (eds) *Petroleum Basins of South America*. AAPG Memoir 62, pp 207–230
- Sempere T, Butler RF, Richards DR, Marshall LG, Sharp W, Swisher CC III (1997) Stratigraphy and chronology of Upper Cretaceous–lower Paleogene strata in Bolivia and northwest Argentina. *Geol Soc Am Bull* 109(6):709–727
- Sillitoe RH, McKee EH (1996) Age of supergene oxidation and enrichment in the Chilean Porphyry Copper Province. *Econ Geol*, 164–179
- Silva González P (2004) Das Süd-Altiplano-Becken (Bolivien) im Tertiär: sedimentäre Entwicklung und tektonische Implikationen. PhD thesis, Freie Universität Berlin
- Springer M (1996) Die regionale Oberflächenwärmeflußdichte-Verteilung in den zentralen Anden und daraus abgeleitete Temperaturmodelle der Lithosphäre. PhD thesis, Freie Universität Berlin
- Springer M, Förster A (1998) Heat-flow density across the Central Andean subduction zone. *Tectonophysics* 291:123–139
- Tatsumi Y, Eggins S (1995) *Subduction zone magmatism*. Blackwell Scientific
- Tawackoli S (1999) Andine Entwicklung der Ostkordillere in der Region Tupiza (Südbolivien). *Berliner Geowiss Abh A203*, p 116
- Uba CE, Heubeck C, Hulka C (in press) facies analysis and basin architecture of the Neogene Subandean synorogenic wedge, southern Bolivia. *Sed Petrol*
- Victor P, Oncken O, Glodny J (2004) Uplift of the western Altiplano plateau: evidence from the Precordillera between 20° and 21°S (northern Chile). *Tectonics* 23: doi 10.1029/2003TC001519
- Wagner G, Van der Haute P (1992) *Fission-track dating*. Kluwer Academic Publishers
- Whitman D, Isacks BL, Chatelain JL, Chiu JM, Perez A (1992) Attenuation of high-frequency seismic waves beneath the Central Andean plateau. *J Geophys Res* 97(B13):19929–19947
- Wigger PJ, Schmitz M, Aranedo M, Asch G, Baldzuhn S, Giese P, Heinsohn, WD, Eloy M, Ricaldi E (1994) Variation in the crustal structure of the Southern Central Andes deduced from seismic refraction investigations. In: Reutter K-J, Scheuber E, Wigger P (eds) *Tectonics of the Southern Central Andes*. Springer-Verlag, Berlin Heidelberg New York, pp 23–48
- Wörner G, Lezaun J, Beck A, Heber V, Lucassen F, Zinngrebe E, Rössling R, Wilke HG (2000) Precambrian and early Paleozoic evolution of the Andean basement at Belén (northern Chile) and Cerro Uyarani (western Bolivian Altiplano). *J S Am Earth Sci* 13:717–737

